Strong magnetic fluctuations in transition metal oxides (invited)

C. Broholm
Department of Physics and Astronomy, The Johns Hopkins University, Baltimore, Maryland 21218 and National Institute of Standards and Technology, Gaithersburg, Maryland 20899

G. Aeppli
AT&T Bell Laboratories, Murray Hill, New Jersey 07974

S.-H. Lee and W. Bao
Department of Physics and Astronomy, The John Hopkins University, Baltimore, Maryland 21218

J. F. DiTusa
Department of Physics and Astronomy, Louisiana State University, Baton Rouge, Louisiana 70803

Most magnets have long-range magnetic order when the thermal energy is less than the local magnetic exchange energy ($T<|\Theta_{CW}|$). Effects such as reduced dimensionality and frustration, however, can suppress the ordering transition and lead to unusual cooperative paramagnetic phases at low temperatures. We review neutron scattering experiments exploring such short-range-ordered phases in insulating transition metal oxides. We discuss $(V_{1-x}Cr_x)_2O_3$, in which orbital fluctuations appear to limit spin correlations to within small ''molecular'' clusters, $SrCr_{9p}Ga_{12-9p}O_{19}$, in which geometrical frustration allows local anitferromagnetic constraints to be fulfilled without long-ranged order, and Y_2BaNiO_5, in which magnetic interactions occur only within chains of spins which are unable to order because of the Haldane effect. Emphasis is placed on the common features of exchange interactions in these oxides and the important role which magnetic neutron scattering has played in understanding the unusual magnetic phenomena. [S0021-8979(96)72208-6]

I. INTRODUCTION

A common structural unit in magnetism is a transition series cation surrounded by six oxygen ions at the vertices of an octahedron.[1] This unit, for example, is the source of interacting magnetic moments in classical three-dimensional antiferromagnets such as MnO, FeO, CoO, NiO, Fe_2O_3, and Cr_2O_3. Adjoining octahedra, however, can also build periodic structures whose connectivity is not conducive to the development of conventional long-ranged order, and therefore may give rise to novel cooperative magnetic phenomena. In this article we review experiments examining such magnetic oxides which have strong magnetic fluctuations and short-ranged spin correlations even at low temperatures ($T \ll \Theta_{CW}$).

The neutron scattering techniques pioneered by Shull and Brockhouse are irreplaceable tools for elucidating spin correlations in these systems, much as they were for conventional Néel antiferromagnets.[2] The measured quantity is the probability that a neutron with a wave vector $\mathbf{k}_i$ is scattered into a final state with wave vector $\mathbf{k}_f$ through its interaction with the sample. Under suitable conditions this scattering process may be treated in the Born approximation, and in this case the scattering probability distribution is proportional to the neutron scattering cross section, which depends only on wave vector transfer, $\mathbf{Q}=\mathbf{k}_i-\mathbf{k}_f$, and energy transfer, $\hbar\omega=(\hbar^2/2m)(k_i^2-k_f^2)$. Here we consider only the magnetic part of the scattering cross section, which is proportional to

$$I_m(\mathbf{Q},\omega)=\sum_{\alpha\beta}(\delta_{\alpha\beta}-\hat{Q}_\alpha\hat{Q}_\beta)S^{\alpha\beta}(\mathbf{Q},\omega), \tag{1}$$

where $S^{\alpha\beta}(\mathbf{Q},\omega)$ is the dynamical spin correlation function,

$$S^{\alpha\beta}(\mathbf{Q},\omega)=|F(Q)|^2\frac{(g\mu_B)^2}{2\pi\hbar}\int dt e^{i\omega t} \times\frac{1}{N}\sum_{\mathbf{R}\mathbf{R}'}\langle S^\alpha_{\mathbf{R}}(t)S^\beta_{\mathbf{R}'}(0)\rangle e^{-i\mathbf{Q}\cdot(\mathbf{R}-\mathbf{R}')}, \tag{2}$$

which contains unique information about magnetic correlations in the sample. In this expression $F(Q)$ is the magnetic form factor, a property of the $3d$ orbitals.[17]

For powder samples the information available from magnetic neutron scattering is less specific than for single crystals, because the scattered intensity only depends on $Q=|\mathbf{k}_i-\mathbf{k}_f|$ and is proportional to the spherically averaged dynamic spin correlation function

$$\langle S(Q,\omega)\rangle=\int\frac{d\Omega_{\hat{Q}}}{4\pi}\frac{1}{2}I_m(\mathbf{Q},\omega). \tag{3}$$

Nonetheless, as we shall see, important results may still be extracted, especially in the small Q limit or when we are interested in Brillouin zone averaged quantities.

For comparison with bulk measurements, and between different neutron scattering experiments, we have in most cases measured scattering cross sections in absolute units. The scale factor between the detector count rate and the quantities of Eqs. (1)–(3) were determined by normalizing to count rates associated with known nuclear scattering cross sections of the samples.

II. ORBITAL FLUCTUATIONS IN $(V_{1-x}Cr_x)_2O_3$?

V_2O_3 can be insulating or metallic and antiferromagnetic or paramagnetic depending on temperature, pressure, and exact stoichiometry,[3] and consequently the material has been a testing ground for theories of electronic correlations and

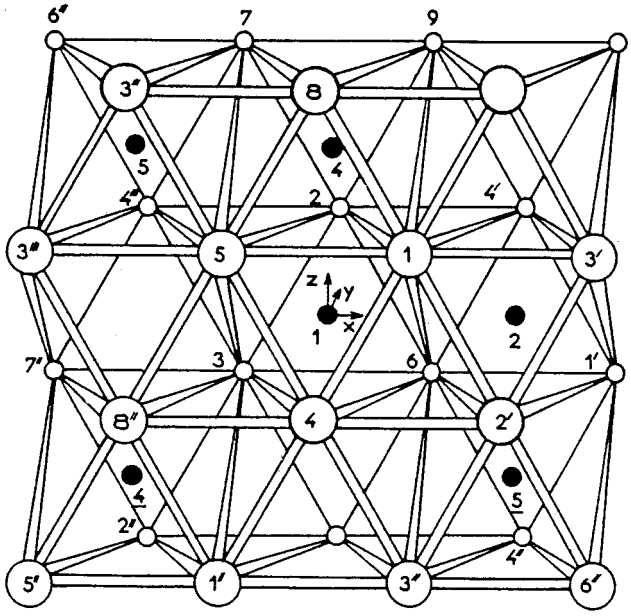

FIG. 1. Crystalline structure of $(V_{1-x}Cr_x)_2O_3$. The trivalent cations (filled circles) are surrounded by O^{2-} ions (open circles) on the vertices of trigonally distorted octahedra. (From Ref. 11.)

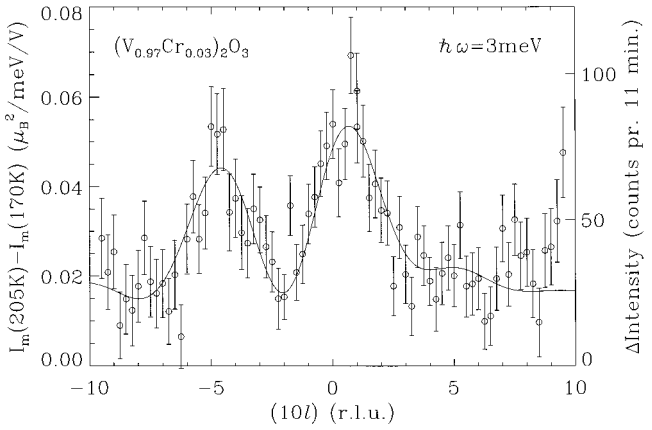

FIG. 2. **Q** dependence of inelastic scattering at $\hbar\omega=3$ meV and $T=205$ K in the paramagnetic insulating phase of $(V_{0.97}Cr_{0.03})_2O_3$. The 170 K data from the antiferromagnetic phase are a good measure of background and were subtracted from the 205 K data. The data were taken on BT2 at NIST with $E_f=13.7$ meV and collimations $60'-40'-40'-60'$ around the PG(002) monochromator and analyzer. A 1-in.-thick PG filter followed the sample.

magnetism for decades.[4,5] Here we shall confine our attention to the insulator $(V_{0.97}Cr_{0.03})_2O_3$ whose antiferromagnetism defies explanation in terms of a conventional Heisenberg spin Hamiltonian.

Figure 1 shows a sketch of the corundum structure of V_2O_3. The trivalent cation sites, which are surrounded by six oxygen atoms on the vertices of trigonally distorted octahedra, form puckered honeycomb layers stacked in such a way that each vanadium site has a nearest neighbor above or below it. V^{3+} has only two $3d$ electrons which occupy the crystal field triplet t_{2g}. The t_{2g} orbitals have significant overlap only with their counterparts on neighboring vanadium atoms and this has two important consequences: (1) V_2O_3 is a Mott insulator as opposed to a charge transfer insulator. (2) Direct cation–cation overlap between in-plane nearest neighbors and the one out-of-plane nearest neighbor are the dominant sources of magnetic exchange interactions.[1] Even though these interactions would appear to yield a three-dimensional nonfrustrated antiferromagnet, the magnetic transition which takes place at $T_N=180$ K, is unusual because (1) it occurs far below $|\Theta_{CW}|=350$ K, (2) it involves an antiferromagnetic structure[6] which is unique for corundum transition metal oxides[2,7,8], (3) it is accompanied by a lattice distortion, and (4) it is a first order transition.

To explore this unusual magnetic phase transition, we have examined spin correlations in the paramagnetic phase by inelastic magnetic neutron scattering. Figure 2 shows the wave vector dependence of neutron scattering at $T=205$ K and $\hbar\omega=3$ meV. For **Q** along the (10l) direction we find two well-defined peaks which, in being almost as wide as the projection of the first Brillouin zone in that direction, imply that magnetic correlations involve only nearest neighbors. The data are qualitatively different from those derived from paramagnetic scattering in conventional three-dimensional antiferromagnets, not only because the correlations are so short ranged for $T/T_N-1=0.08$, but also because coherent scattering dominates over incoherent scattering despite the very short correlation lengths. Correlations are so short ranged, in fact, that we can fit the data to a truncated lattice sum which neglects all but the correlations between nearest neighbors,

$$S(\mathbf{Q})=\sum_{\mathbf{RR'}}\langle S_{\mathbf{R}}S_{\mathbf{R'}}\rangle\exp[i\mathbf{Q}\cdot(\mathbf{R}-\mathbf{R'})]. \tag{4}$$

The best fit, which also describes $(h,0,-5)$ and $(h01)$ scans at $\hbar\omega=3$ meV, is shown as a solid line in Fig. 2. From the fit we obtain values for nearest-neighbor spin correlations: $\langle\mathbf{S}_{[0,0,0]}\cdot\mathbf{S}_{\langle 0,0,1/6+\delta\rangle}\rangle=0.6(3)$, $\langle\mathbf{S}_{[0,0,0]}\cdot\mathbf{S}_{\langle 1/3,2/3,\delta\rangle}\rangle=-0.19(8)$, $\langle\mathbf{S}_{[0,0,0]}\cdot\mathbf{S}_{\langle 1/3,2/3,\delta-1/6\rangle}\rangle=0.18(8)$, and $\langle\mathbf{S}_{[0,0,0]}\cdot\mathbf{S}_{\langle 1/3,2/3,1/6\rangle}\rangle=-0.09(3)$ where $\delta=0.026$. These values were normalized so that $\langle\mathbf{S}_{[0,0,0]}\cdot\mathbf{S}_{[0,0,0]}\rangle=1$. Figure 3 shows that it is not a lack of interactions that prevents longer-ranged correlations from developing. The full widths at half-maximum (FWHM) of constant–$\hbar\omega$ scans along the (10l) direction through the peak at $\mathbf{Q}\approx(101)$ are almost indistinguishable from those at $\hbar\omega=3$ meV, for energy transfers, $\hbar\omega$, as high as 18 meV. Also the nearly $\hbar\omega$-independent peak amplitudes indicate that these correlations may persist to even higher energies.

The **Q** dependence of paramagnetic scattering from $(V_{1.97}Cr_{0.03})_2O_3$ resembles that of energy integrated scattering from isolated spin clusters in dilute magnets.[9] However, the energy spectrum is continuous indicating that we are dealing with excitations in a macroscopic physical system. A possible explanation for this unusual behavior was recently proposed by Rice.[10] His idea is that orbital fluctuations in the paramagnetic phase of $(V_{1-x}Cr_x)_2O_3$ inhibit long-ranged spin correlations through their effect on exchange interactions. In his description, which is based on the work of Castellani *et al.*,[11] one d electron is occupied in covalent bonding with the out-of-plane nearest neighbor while the other must choose which of the three in-plane vanadium neighbors to bond with. Pairs which bond have ferromagnetic spin–spin

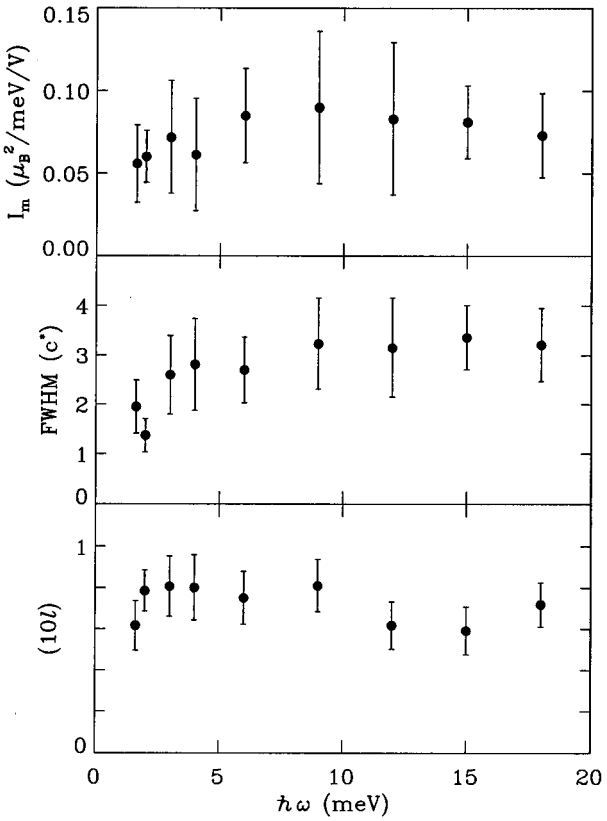

FIG. 3. $\hbar\omega$ dependence of inelastic scattering for $\mathbf{Q}\approx(101)$ at $T=205$ K in $(V_{0.97}Cr_{0.03})_2O_3$ as derived from Lorentzian fits to constant $\hbar\omega$ scans along the $(10l)$ direction. The top frame is the amplitude of the modulated component, the middle frame is the FWHM, and the bottom frame is the peak position.

interaction whereas those which do not interact antiferromagnetically, and this leads to an effective spin–orbit coupling which cannot be accounted for by a conventional spin Hamiltonian. In this theory the coupling of the spin system to orbital fluctuations is what inhibits the development of spin order for $T\approx|\Theta_{CW}|$ and the magnetic transition is actually driven by an orbital ordering transition. In particular, the orbital order enables the development of long-ranged spin order by establishing an ordered array of spin exchange interactions. Further neutron scattering experiments probing the effects of orbital fluctuations on spin fluctuations both in the low and high temperature phases are underway to test this hypothesis.

III. ISOLATED SPIN PAIRS AND FRUSTRATION IN $SrCr_{9p}Ga_{12-9p}O_{19}$

$SrCr_{9p}Ga_{12-9p}O_{19}$ is a more complicated substance than most condensed matter physicists are normally willing to consider. Nonetheless, the unique magnetic properties of this insulating oxide do warrant attention. The bulk properties which called our attention to $SrCr_{9p}Ga_{12-9p}O_{19}$ were (1) a magnetic susceptibility which follows Curie–Weiss behavior with $\Theta_{CW}=-500$ K down to $T\approx100$ K,[12] (2) the absence of static order until a spin-glass-like transition at $T_g=3.5$ K$\ll|\Theta_{CW}|$,[13] and (3) low temperature specific heat data,

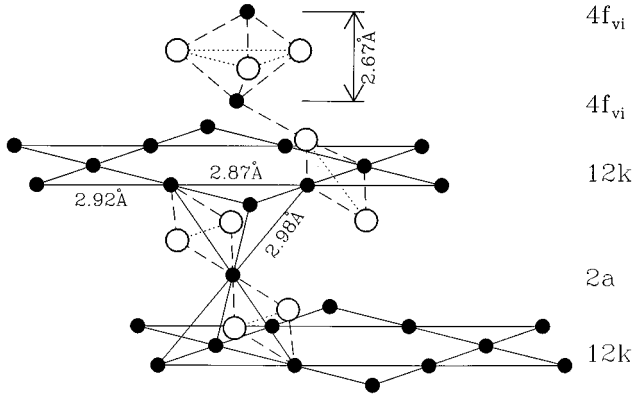

FIG. 4. Chromium ions (solid circles) and part of their distorted O^{2-} octahedral coordination in $SrCr_{9p}Ga_{12-9p}O_{19}$. (From Ref. 16.)

$C(T)$, which in being proportional to T^2 resembles a long-range ordered two-dimensional magnet more than a conventional spin glass for which $C\propto T$.[13]

The aspects of the crystal structure which are relevant for this discussion are shown in Fig. 4. As in V_2O_3, the trivalent magnetic cation, in this case Cr^{3+}, is surrounded by a distorted octahedron of oxygen atoms. The cation lattice is however more complicated in this case, encompassing three distinct sites which are denoted $12k$, $2a$, and $4f_{vi}$. The $12k$ layer is a slightly distorted Kagomé lattice whereas the $2a$ and $4f_{vi}$ layers are triangular lattices. The Cr^{3+} ions in the $12k-2a-12k$ block form corner-sharing tetrahedra, as in three-layer (111) slabs of the trivalent cation sites in the cubic pyrochlore[14,15] and spinel structures.

Neutron scattering experiments have enabled us to derive a comprehensive model of magnetic interactions in this material, and to identify the three-layer $12k-2a-12k$ slab as the origin of the two-dimensional frustrated magnetism in $SrCr_{9p}Ga_{12-9p}O_{19}$.[16] Figure 5 shows wave vector integrated inelastic neutron scattering, $S(\omega)$, at $T=1.3$ K from a powder sample of $SrCr_{9p}Ga_{12-9p}O_{19}$ with $p=0.92(5)$. Apart

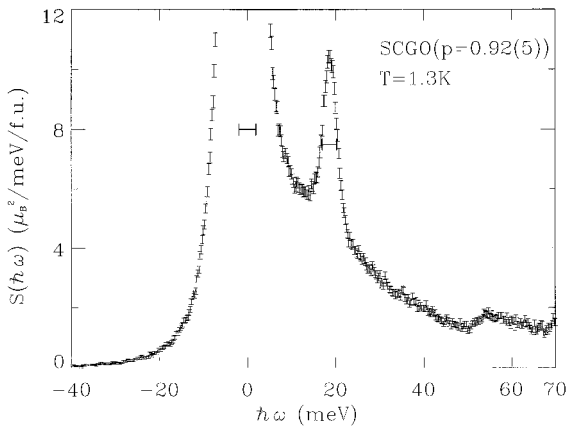

FIG. 5. Energy dependence of wave-vector-integrated magnetic neutron scattering $S(\hbar\omega)=\int[I(Q,\omega)/|F(Q)|^2]Q^2dQ/\int Q^2dQ$ from $SrCr_{9p}Ga_{12-9p}O_{19}$, $p=0.92(5)$ at $T=1.3$ K. The data were obtained from 1139 μA h of beam time on the HET instrument at ISIS with $E_i=100$ meV using slit pack C rotating at 100 Hz. The horizontal bars show the FWHM of the instrumental resolution. (From Ref. 16.)

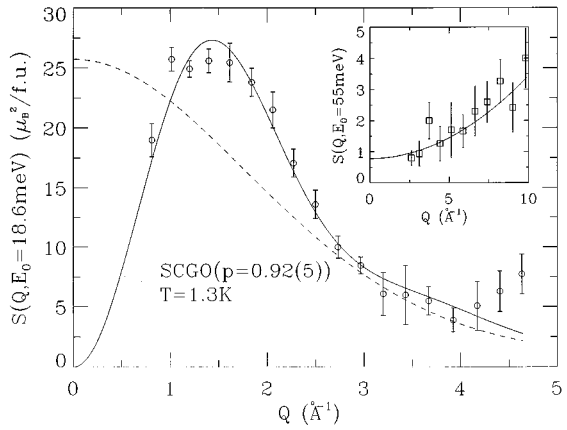

FIG. 6. Q dependence of the integrated intensity of the 20 meV excitation in $SrCr_{9p}Ga_{12-9p}O_{19}$, $p=0.92(5)$ at $T=1.3$ K. The dashed line is the magnetic form factor squared for chromium (Ref. 17), the solid line was calculated for 0.7(1) antiferromagnetically interacting pairs of spins per formula unit. The inset identifies the 55 meV feature visible in Fig. 5 as a vibrational in origin because the integrated intensity rises with wave vector transfer. The data were obtained using the MARI instrument at ISIS (Ref. 16).

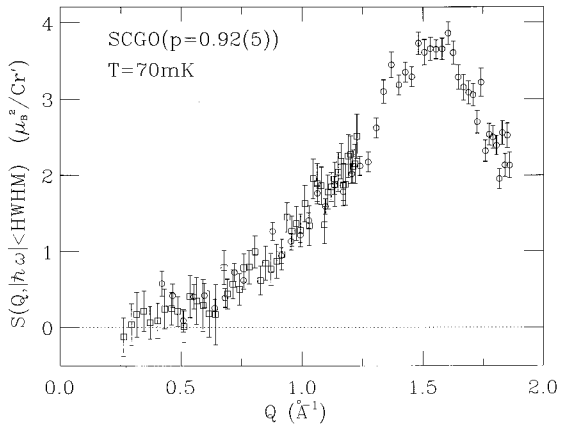

FIG. 7. Q dependence of elastic magnetic scattering from $SrCr_{9p}Ga_{12-9p}O_{19}$, $p=0.92(5)$ at $T=70$ mK. The data were obtained by subtracting elastic peak intensities at $T=20$ K from the same at $T=70$ mK. The experiment was performed on the IRIS instrument at ISIS using both its PG(002) analyzer (open circles) and its MICA(004) analyzer (open squares). (From Ref. 20.)

from the incoherent elastic peak and a broad spectrum of magnetic scattering visible from 0 to 40 meV, we notice a resolution limited peak at $\hbar\omega=18.6$ meV. Because the peak is sharp in wave-vector-integrated data, it must be associated with a nondispersive excitation and is therefore likely to arise from single atoms, or small clusters of atoms, which are decoupled from the rest of the system. From the Q dependence of the energy-integrated intensity of the ridge, shown in Fig. 6, we can exclude that it arises from (i) a local vibrational excitation, because the intensity decreases with Q and (ii) a crystal field excitation on a single chromium atom, because the Q dependence is distinguishable from the magnetic form factor for chromium.[17] Instead, the Q dependence of the scattering closely resembles that from an isolated pair of antiferromagnetically interacting spins,[9] shown as a solid line in Fig. 6. Such spin pairs also provide a detailed account for the energy and temperature dependence of the data, including a peak in $S(\omega)$ at $\hbar\omega=37.2$ meV which only appears for $T>100$ K.[16]

Considering also the values of the two fitting parameters which went into calculating the solid line in Fig. 6 and the position of the peak in Fig. 5, we conclude that there are 0.7(1) isolated spin pairs per formula unit in $SrCr_{9p}Ga_{12-9p}O_{19}$ $[p=0.92(5)]$. Spins of a pair are separated by $R\approx 2.68(7)$ Å and interact antiferromagnetically with an exchange coupling constant $J=18.6(1)$ meV. Since $4f_{vi}$ spins are the only spins which each are part of a unique spin pair, and since there are 0.78 $4f_{vi}$–$4f_{vi}$ spin pairs per formula unit separated by 2.681(3) Å in our sample, it is likely that the $4f_{vi}$ Cr^{3+} ions are the ones forming isolated spin pairs in $Sr\,Cr_{9p}Ga_{12-9p}O_{19}$.

The oxygen octahedra of chromium ions in adjacent $4f_{vi}$ planes share a common face whereas the oxygen octahedra of neighboring $4f_{vi}$ and $12k$ sites share a corner. The exact same environment exists in corundum Cr_2O_3 where it has been established[18] that the exchange constant between Cr^{3+} ions with corner sharing oxygen octahedra is only 0.2 meV because occupied $3d$ orbitals in Cr^{3+} do not overlap oxygen orbitals.[1] Occupied orbitals of Cr^{3+} ions in face sharing octahedra, however, have appreciable direct overlap which in Cr_2O_3 gives rise to a 15 meV antiferromagnetic exchange coupling. This number, being close to the 18.6 meV exchange constant for spin pairs in SCGO $[p=0.92(5)]$, supports our comparison to Cr_2O_3 and our conclusion that $4f_{vi}$ spin pairs form isolated singlets in $SrCr_{9p}Ga_{12-9p}O_{19}$.

Having accounted for the $4f_{vi}$ chromium sites we are left with the quasi-two-dimensional magnet consisting of a triangular lattice $(2a)$ sandwiched between two Kagomé lattices $(12k)$. Alternatively this lattice can be described as a three-layer (111) slab of the trivalent cation sites in the cubic pyrochlore or spinel structures. The oxygen octahedra of nearest neighbors within this spin system all share an edge and exchange interactions are therefore expected to be comparable in magnitude. Fitting high temperature bulk susceptibility data to the sum of the susceptibility of the $4f_{vi}$ spin pairs and a Curie–Weiss term to account for the pyrochlore slab, we extract a value of 9.5(5) meV for the average exchange constant within the slab. It is satisfying that this number is close to the value of 6.7(4) meV measured for the exchange constant between chromium ions whose octahedra share an edge in Cr_2O_3.[18]

Evidently it is the reduced dimensionality and unique connectivity within this three-layer magnetic which give rise to the unusual cooperative magnetic properties of $SrCr_{9p}Ga_{12-9p}O_{19}$. We have performed a number of neutron scattering experiments to explore these properties.[19] Our most interesting data are perhaps those establishing the Q dependence of elastic magnetic scattering in the spin glass phase.[20] The data, shown in Fig. 7, were obtained by subtracting elastic scattering at $T=20$ K$>T_g$ from the same at $T=70$ mK. Since the half-width at half-maximum (HWHM) of the energy resolution function in this experiment was 7.5 μeV (circles) and 2.25 μeV (squares) this measurement probes magnetic correlations which persist on the nanosecond time scale. From the wave vector integral of the data we

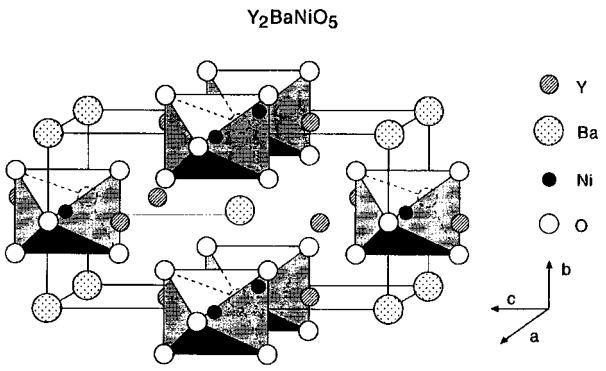

FIG. 8. Structure of Y_2BaNiO_5. The oxygen ion which is a member of the octahedral coordination of two nickel ions mediates superexchange along the spin chain. (From Ref. 31.) Holes reside on this atom for $Y_{1.90}Ca_{0.10}BaNiO_5$.

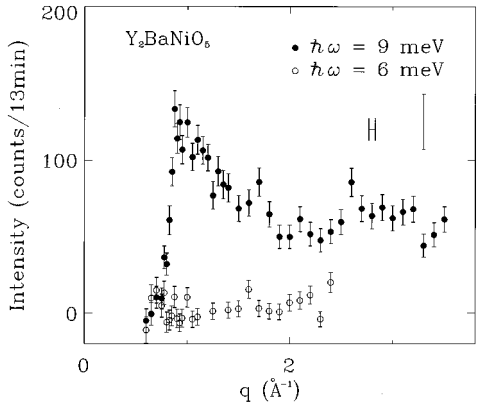

FIG. 9. Q dependence of inelastic magnetic scattering from a powder sample of Y_2BaNiO_5 at $T=10$ K for $\hbar\omega=6$ meV (open circles) and $\hbar\omega=9$ meV (filled circles). Background was measured for each of these scans at $\hbar\omega=-6$ and -9 meV, respectively, and subtracted. The horizontal bar corresponds to the FWHM Q resolution. The experiment was performed on the thermal neutron triple axis spectrometer BT2 at NIST with $E_i=40.3$ meV and collimations $60'-20'-42'-44'$ around the PG(002) monochromator and analyzer. A 2-in.-thick PG filter preceded the monochromator. (Adapted from Ref. 32.)

conclude that the frozen moment in this system is only $1.9(2)\mu_B$, which is less than half of the frozen moment in a conventional Neél state formed by $S=3/2$ Cr^{3+} ions and thus implies that quantum spin fluctuations are strong in this insulating magnet. The elastic magnetic scattering is also unusual in that although we are dealing with a concentrated magnet with only weak structural disorder, there are no sharp peaks in the data, implying that long-ranged magnetic correlations are absent. Instead the broad peak at wave vector $Q\approx1.5$ Å^{-1} indicates the presence of short-range antiferromagnetic correlations. Since the width of the peak is comparable to its displacement from $Q=0$ static magnetic correlations are only maintained between nearest neighbors. Nonetheless, $S(Q)$ appears to vanish as $Q\rightarrow0$. A vanishing forward cross section is very significant, because it implies that there exists a decomposition of the frozen spin state into subgroups of spins which possess net spin zero. The zero spin subgroups could be pairs, triangles, or tetrahedra of nearest-neighbor Cr^{3+} ions. Although such a spin configuration in principle could be concocted on most lattices, it appears to be the unique connectivity of the pyrochlore slab which makes such a spin configuration energetically favorable by allowing for all antiferromagnetic interactions to be satisfied without establishing long-ranged order. In this respect the frozen spin configuration in $SrCr_{9p}Ga_{12-9p}O_{19}$ resembles the ground state of the weakly diluted classical Kagomé antiferromagnet which Shender *et al.*[21] have found to obey a "rule of satisfied triangles."

IV. HALDANE GAP AND HOLE DOPING IN Y_2BaNiO_5

The combination of low dimensionality and a low integer spin quantum number ($S=1$) causes Y_2BaNiO_5 to be a rare example of a transition metal oxide which evades magnetic order down to temperatures as low as 50 mK.[22] One dimensionality in this material comes about because oxygen octahedra, which coordinate Ni^{2+}, share a corner only for Ni^{2+} ions displaced along the a axis. Because Ni^{2+} ($3d^8$) has more than three $3d$ electrons, the superexchange interactions between such magnetic cations are strong,[1] and by dominating over all other exchange interactions, yield a one-dimensional antiferromagnet (see Fig. 8).

The consequences of this microscopic solid state chemistry for the magnetic properties of the material are quite astonishing. Figure 9, for example, shows the Q dependence of inelastic neutron scattering from a powder sample for $T=10$ K$\ll|\Theta_{CW}|$ K[23] and $\hbar\omega=9$ meV$\ll k_B|\Theta_{CW}|$. In this low T and $\hbar\omega$ regime, neutron scattering from a conventional three-dimensional Heisenberg antiferromagnetic is strongest at low energies and always peaked for Q in the vicinity of magnetic Bragg peaks. For Y_2BaNiO_5, however, inelastic scattering is only visible in the higher energy Q scan ($\hbar\omega=9$ meV) and only beyond a sharp onset at $Q=0.85$ Å$^{-1}\approx\pi/a$. Beyond this value no pronounced Q dependence is visible in the data except for a gradual decrease in intensity as Q increases. The absence of well-defined peaks in constant energy scans implies that long-ranged three-dimensional spin correlations do not exist in this material. However, the resolution limited onset of scattering as a function of Q distinguishes this magnet from conventional short-range ordered paramagnets, and indicates the presence of some form of long-ranged one-dimensional coherence.[24]

The unusual absence of inelastic scattering at $\hbar\omega=6$ meV was further explored through a constant $Q=1.1$ Å^{-1} scan (Fig. 10) which shows clear evidence of a 9 meV gap in the magnetic excitation spectrum. The single ion anisotropy of octahedrally coordinated Ni^{2+} cannot account for the gap, which instead appears to be an experimental example of the so-called Haldane gap[25] which characterizes the excitation spectrum of integer spin, one-dimensional antiferromagnets.[26,27] It is interesting to note that this quantum many-body effect actually prevents magnetic order from taking place at any temperature in real materials such as Y_2BaNiO_5 and NENP[28] in which residual three-dimensional interactions do not exceed the threshold required to drive the gap to zero as they do in $CsNiCl_3$.[26]

What sets Y_2BaNiO_5 apart from other quasi-one-dimensional magnets previously studied is that holes may be

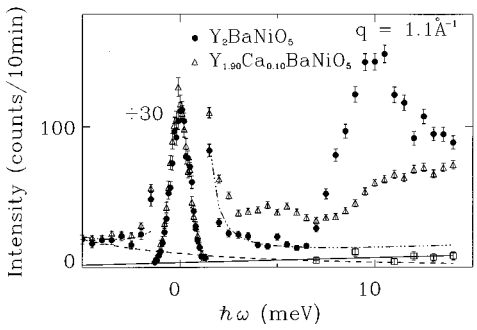

FIG. 10. $\hbar\omega$ dependence of inelastic neutron scattering at wave vector transfer $Q=1.1$ Å$^{-1}=0.65a^*$ and temperature, $T=10$ K. Solid circles are for Y_2BaNiO_5, open triangles for $Y_{1.90}Ca_{0.10}BaNiO_5$, a material where holes are placed on the superexchange mediating oxygen ions with a mean separation of 10 nickel sites. The data were obtained on the thermal neutron triple axis spectrometer BT2 at NIST with $E_f=14.7$ meV and collimations $60'-20'-42'-44'$ around the PG(002) monochromator and analyzer. A 1-in.-thick PG filter followed the sample. The solid line is the background measured with analyzer turned 10° from reflection. The dashed line is the background resulting from $\lambda/2$ neutrons in the unfiltered incident beam. The dashed–dotted line shows the tails of the elastic signal superimposed on the previously mentioned background contributions. The sharp peak centered at $\hbar\omega=0$ comes from incoherent elastic nuclear scattering. Adapted from (Ref. 29.)

placed on the superexchange mediating oxygen atoms of the $(NiO_5)^{8-}$ chains by substituting Ca^{2+} for Y^{3+}.[29] This leads to a simple yet novel many-body system: Charge carriers interacting with a quantum spin liquid. The open triangles in Fig. 10 show that hole doping both introduces a subgap resonance in the excitation spectrum and shifts spectral weight above the gap to higher energies. Whereas the latter effect is also seen in samples where the average chain length is reduced by replacing Ni^{2+} by Zn^{2+}, the subgap resonance is peculiar to hole-doped samples. The simplest model which may be relevant for understanding the subgap resonance treats holes as static perturbations in the superexchange. In the analogous phonon problem a localized perturbation of interactions leads to a bound state or localized ''optical'' mode. A recent theoretical analysis of such a model has indeed identified a subgap resonance pinned to the middle of the Haldane gap when the impurity bond strength modulation exceeds a certain threshold.[30]

ACKNOWLEDGMENTS

We would like to acknowledge our collaborators in this work M. A. Adams, C. J. Carlile, S. A. Carter, C. T. Chen, S.-W. Cheong, B. Hessen, J. M. Honig, T. J. L. Jones, P. Metcalf, J.-H. Park, T. G. Perring, A. P. Ramirez, T. F. Rosenbaum, J. Spalek and, S. F. Trevino. We also thank the ISIS facility at the Rutherford Appleton Laboratory, and the National Institute of Standards and Technology for providing the experimental facilities which enabled the research, and the National Science Foundation which funded work at JHU through Grant Nos. DMR-9302065, DMR-9357518, and DMR-9453362.

[1] J. B. Goodenough, Phys. Rev. **117**, 1442 (1960), Prog. Solid State Chem. **5**, 145 (1972).
[2] C. G. Shull, W. A. Strauser, and E. O. Wollan, Phys. Rev. **83**, 333 (1951).
[3] D. B. McWhan, A. Menth, J. P. Remeika, W. F. Brinkman, and T. M. Rice, Phys. Rev. B **7**, 1920 (1973).
[4] N. F. Mott, *Metal Insulator Transitions* (Taylor & Francis, London, 1974).
[5] W. F. Brinkman and T. M. Rice, Phys. Rev. B **2**, 4302 (1970).
[6] R. M. Moon, Phys. Rev. Lett. **25**, 527 (1970).
[7] D. E. Cox, W. J. Takei, and G. Shirane, J. Phys. Chem. Solids **24**, 405 (1963).
[8] E. F. Bertaut, Compt. Rend. Acad. Sci. **252**, 76 (1961).
[9] A. Furrer and H. U. Güdel, J. Magn. Magn. Mater. **14**, 256 (1979).
[10] T. M. Rice (unpublished).
[11] C. Castellani, C. R. Natoli, and J. Ranninger, Phys. Rev. B **18**, 4945, (1978).
[12] X. Obradors, A. Labarta, A. Isalgue, J. Tejada, J. Rodriguez, and M. Pernet, Solid State Commun. **65**, 189 (1988).
[13] A. P. Ramirez, G. P. Espinosa, and A. S. Cooper, Phys. Rev. Lett. **64**, 2070 (1990); Phys. Rev. B **45**, 2505 (1992).
[14] M. J. Harris, M. P. Zinkin, Z. Tun, B. M. Wanklyn, and I. P. Swainson, Phys. Rev. Lett. **73**, 189 (1994).
[15] J. N. Reimers, J. E. Greedan, R. K. Kremer, E. Gmelin, and M. A. Subramanian, Phys. Rev. B **43**, 3387 (1991); J. E. Greedan, J. N. Reimers, C. V. Stager, and S. L. Penny, *ibid*. **43**, 5682 (1991).
[16] S.-H. Lee, C. Broholm, G. Aeppli, T. G. Perring, B. Hessen, and A. Taylor (unpublished).
[17] A. J. Freeman and R. E. Watson, Acta. Crystallog. **14**, 231 (1961).
[18] E. J. Samuelsen, M. T. Hutchings, and G. Shirane, Physica **48**, 13 (1970).
[19] C. Broholm, G. Aeppli, G. P. Espinosa, and A. S. Cooper, Phys. Rev. Lett. **65**, 3173 (1990); J. Magn. Magn. Mater. **69**, 4968 (1991).
[20] S.-H. Lee, C. Broholm, G. Aeppli, A. P. Ramirez, T. G. Perring, C. J. Carlile, M. A. Adams, T. J. L. Jones, and B. Hessen (unpublished).
[21] E. F. Shender, V. B. Cherepanov, P. C. W. Holdsworth, and A. J. Berlinsky, Phys. Rev. Lett. **70**, 3812 (1993).
[22] A. P. Ramirez, S.-W. Cheong, and M. L. Kaplan, Phys. Rev. Lett. **72**, 3108 (1994).
[23] B. Batlogg, S.-W. Cheong, and L. J. W. Rupp, Jr., Physica **194–196B**, 173 (1994).
[24] M. den Nijs and Koos Rommelse, Phys. Rev. B **40**, 4709 (1989).
[25] F. D. M. Haldane, Phys. Rev. Lett. **50**, 1153 (1983).
[26] Z. Tun, W. J. L. Buyers, R. L. Armstrong, K. Hirakawa, and B. Briat, Phys. Rev. B **42**, 4677 (1990).
[27] L. P. Regnault, J. Rossat-Mignod, J. P. Renard, M. Verdaguer, and C. Vettier, Physica (Amsterdam) **156–157B**, 247 (1989); S. Ma, C. Broholm, D. H. Reich, and B. J. Sternlieb, Phys. Rev. Lett. **69**, 3571 (1992).
[28] O. Avenel, J. Low Temp. Phys. **89**, 547 (1992).
[29] J. F. DiTusa, S.-W. Cheong, J.-H. Park, G. Aeppli, C. Broholm, and C. T. Chen, Phys. Rev. Lett. **73**, 1857 (1994).
[30] Z.-Y. Lu, Z.-B. Su, and L. Yu, Phys. Rev. Lett. **74**, 4297 (1995); other relevant theoretical papers are E. Sørensen and I. Affleck, Phys. Rev. B **51**, 16115 (1995); S. Fujimoto and N. Kawakami, *ibid*. **52**, 6189 (1995); K. Penc and H. Shiba, *ibid*. **52**, R715 (1995); E. Dagotto, J. Riera, A. Sandvik, and A. Moreo (unpublished).
[31] D. J. Buttrey, J. D. Sullivan, and A. L. Rheingold, J. Solid State Chem. **88**, 291 (1990).
[32] J. F. DiTusa, S.-W. Cheong, C. Broholm, G. Aeppli, L. W. Rupp, Jr., and B. Batlogg, Physica B **194–296**, 181 (1994).